24 Observations of the atmospheric boundary layer in Rondônia

C.A. NOBRE[1], G. FISCH[2], H.R. da ROCHA[3], R.F. da F. LYRA[4], E.P. da ROCHA[5], A.C.L. da COSTA[5] and V.N. UBARANA[6]

[1] *Instituto Nacional de Pesquisas Espaciais, São José dos Campos, Brazil*
[2] *Centro Técnico Aeroespacial, São José dos Campos, Brazil*
[3] *Universidade de São Paulo, São Paulo, Brazil*
[4] *Universidade Federal de Alagoas, Maceió, Brazil*
[5] *Universidade Federal do Pará, Belém, Brazil*
[6] *Fund. Cearence de Meteorologia e Rec. Hídricos, Fortaleza, Brazil*

INTRODUCTION

Throughout the last decade, the Amazon region has received worldwide attention because of its mineral riches, its great biodiversity and the effects that deforestation may provoke on climate at regional and global scales. Determining the climatic effects of Amazonian deforestation has been the subject of many general circulation model (GCM) experiments over the past few years, for example Dickinson and Henderson-Sellers (1988), Lean and Warrilow (1989), Nobre *et al.* (1991), Lean and Rowntree (1993), Henderson-Sellers *et al.* (1993) and Manzi (1993). All these simulations have agreed that, following total deforestation of the Amazon basin, there would be an increase in air temperature (by 0.6 to 2.0 degrees C), a reduction in precipitation and evaporation (20 to 30%) and the dry season would become longer. Such modifications to the climate would have serious ecological consequences for the Amazon region.

The GCMs used for these numerical simulations contain complex parameterizations of land surface processes (e.g. Dickinson *et al.*, 1984; Sellers *et al.*, 1986; Noilhan and Planton, 1989) to make them as realistic as possible. Much effort is directed at calibrating these parameterizations accurately for different areas of the earth's surface (e.g. Wright *et al.*, 1996). However, the land surface processes and the atmosphere interact strongly to shape the weather and climate of a region. It is, therefore, also important to study the behaviour of the atmospheric boundary layer (ABL) in which these interactions take place, along with the land-surface processes, if GCMs are to be successful in predicting the climate.

The Rondônia Boundary Layer Experiment (RBLE-II) was conceived to collect data on the ABL over two representative surfaces in the Amazon region of Brazil; tropical forest and a deforested, pasture area. Previously, the influence of tropical vegetation on the thermodynamic structure and growth of the boundary layer has been

Amazonian deforestation and climate. Edited by J.H.C. Gash, C.A. Nobre, J.M. Roberts and R.L. Victoria.

addressed by Martin *et al.* (1988), for Manaus in central Amazon only and by Lyra *et al.* (1992) for equatorial Africa. The present paper deals with the observations of ABL growth and decay made during RBLE-II. A companion paper (Fisch *et al.*, 1996) describes some of the modelling aspects of the experiment.

DATA AND SITE

RBLE-II took place in the Ji-Paraná region of Rondônia in the southwest of the Amazonian tropical forest during the 1993 dry season (July). This area was chosen for the experiment because it has a distinct dry season and although it is suffering a high rate of deforestation, large areas of pasture and forest, suitable for boundary layer studies, coexist there (Gash *et al.*, 1996). The RBLE-II sites were the same sites as used for ABRACOS; the forest site was Reserva Jaru (10° 5' S, 61° 55' W, 120 m above sea level) and the pasture site was Fazenda Nossa Senhora da Aparecida (10° 45' S, 62° 22' W, 220 m above sea level). The forest canopy has an average height of 30 m, whilst the vegetation at the pasture site is mostly grass (*Brachiaria brizantha*), which was established 15 years ago and is typical of ranchland in the area. McWilliam *et al.* (1996) give more details about the experimental sites of ABRACOS; Gash*et al.*(1996) give an overview of ABRACOS and describe all the characteristics of vegetation at both sites.

ABL data were taken at both the forest and the pasture sites during the experiment although not simultaneously. At each site, radiosonde and tethered balloon profiles were made at 02.00, 05.00, 08.00, 11.00, 14.00, 17.00, 20.00 and 23.00 h local time. A Vaisala (Finland) radiosounding system was used along with sondes which measure the pressure, air temperature and humidity. The wind speed and direction were determined from the Omega network. These sondes are accurate to 0.1°C for air temperature, 0.1 hPa for atmospheric pressure, 1% for relative humidity, 0.5 m s^{-1} for windspeed and 1 degree for wind direction. The tethered instrument is manufactured by A.I.R. (USA) with a sonde measuring pressure, dry and wet bulb temperatures, windspeed and direction. Its accuracy is 0.1°C for temperature, 0.1 hPa for atmospheric pressure, 0.1 m s^{-1} for windspeed and 1 degree for wind direction. All the data were gathered and stored by a personal computer. To complement the ABL information, an automatic weather station (recording hourly values of air temperature, relative humidity, windspeed and direction, solar and net radiation fluxes and precipitation) and an eddy-correlation instrument (the Institute of Hydrology Hydra: Shuttleworth*et al.*, 1988) recording hourly values of momentum and energy fluxes were also run at both sites throughout the experiment.

As mentioned above, the ABL data were not collected simultaneously at the forest and the pasture sites. For seven days (3 to 10 July 1993) measurements were made at the forest site. This period will be referred to as Phase A. The equipment was then moved to the pasture site for a second seven-day measurement period, Phase B, which lasted from 18 to 25 July 1993. During Phase A, a cold air mass moved across the Ji-Paraná region from the south and modified the atmospheric structure. Such

events, known locally as "friagens", are relatively common in the region. This particular event, and its influence on the atmospheric structure, is analysed in detail by Fisch (1995). In the current analysis, however, data gathered on days affected by the friagem are not considered.

To determine the main characteristics of the structure of the ABL over forest and pasture during the experiment, a composite profile was made for each site . For the pasture site, seven complete days were used in the analysis. Only four days were used in the forest case, however, as between 7 and 9 July the atmospheric structure was strongly influenced by the friagem.

CLIMATOLOGY OF THE JI-PARANÁ REGION

The climatology of the Ji-Paraná region will be discussed briefly, using conventional meteorological data measured at Ouro Prêto D'Oeste. This data-set has been kindly provided by Comissão Executiva da Lavoura do Cacau (CEPLAC). The CEPLAC station is about 20 km from the Fazenda Nossa Senhora site and about 80 km from Reserva Jaru. Figure 1 presents the climatological patterns of rainfall and air temperature for the Ji-Paraná area. Monthly average values are available from 1982 until 1992 and indicate strong seasonality: during the wet period (from November up to April) the monthly precipitation is higher than 200 mm per month. During the dry season (from June until August), the monthly total rarely reaches 20 mm. Usually, in July, the rainfall is less than 5 mm per month. However, during the dry season, there are some cold spells (between May until September there are, on average, seven cases a year, with two or three in July), which on some occasions have associated rainfall. The air temperature also shows seasonality with October (25.5°C) and July (22.6°C) the hottest and coldest months, respectively. October coincides with the end of dry season whilst the average temperature in July is low due to the influence of the friagem.

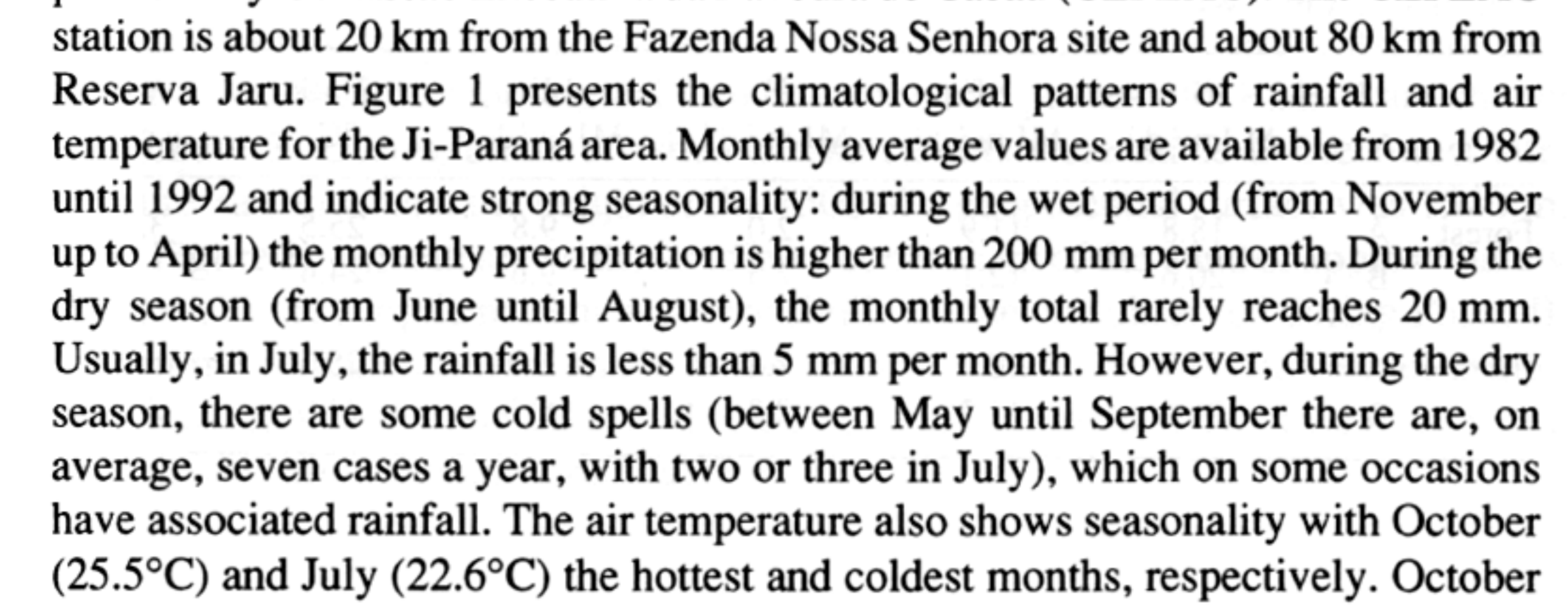

Figure 1 Climatological patterns of rainfall and temperature for the Ji-Paraná area, 1982-1992 (Source: CEPLAC)

MICROMETEOROLOGICAL ASPECTS OF RBLE-II

To characterise the weather patterns during the two phases, an average daily energy budget has been computed for the forest and pasture sites for both Phases A and B (Table 1). So that the average energy budget was calculated from the same number of days in each case, Phase A is considered for these purposes to run from 29 June until 5 July. Phase B has remained unchanged. During Phase A, there was moderate to strong convection with convective cloud cover. During Phase B, the weather in the region was dominated by the influence of a large-scale high pressure area and cloud convection was suppressed. The solar radiation at both sites increased from

Table 1 Average integrated values from fluxes of solar radiation (S), Net-radiation (NET), sensible (H) and latent (LE) heat fluxes, daily average of air temperature (TEMP) and integrated precipitable water (WP).

		S $M.Jm^{-2}\ d^{-1}$	NE $MJ\ m^{-2}\ d^{-1}$	H $MJ\ m^{-2}\ d^{-1}$	LE $MJ\ m^{-2}\ d^{-1}$	TEMP °C	WP $g\ cm^{-2}$
Forest	A	18.8	11.9	2.0	9.8	25.5	3.8
	B	20.6	12.1	2.5	9.6	24.4	
Pasture	A	17.7	10.1	2.7	7.0	25.5	
	B	20.1	11.2	2.2	8.7	24.0	2.6

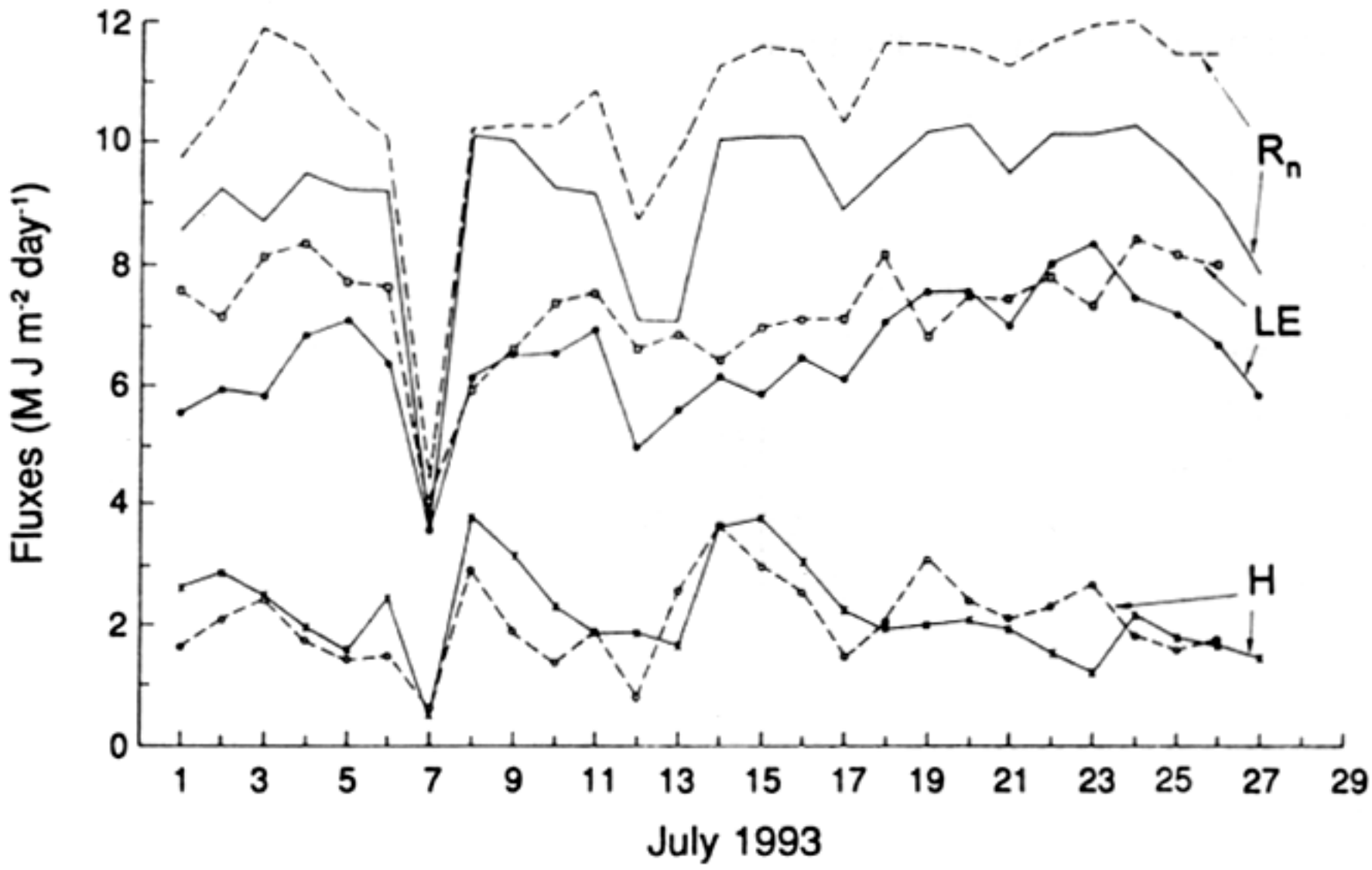

Figure 2 Time series of the components of the energy budget fluxes: net-radiation (Rn), sensible heat (H) and latent heat (LE), at the forest (---) and pasture (—) sites during RBLE-II

Phase A to Phase B, due to the reduced cloud cover. This difference was 10% for the forest and 13% for the pasture site and has led to a different partitioning of energy between the sensible and latent heat fluxes. Figure 2 presents a time series of the components of the energy budget. At the forest site, there was a small increase in net radiation, balanced by an increase in sensible heat and decrease in evapotranspiration. However, at the pasture site, there was a significant increase in net-radiation (11%) together with an increase in evaporation and soil heat flux and a decrease in the sensible heat flux. This increase in evaporation can be explained by the fact that there was precipitation in the preceding week which moistened the soil. There was a decrease in daily average temperature at both sites, but the diurnal curves show an increase in amplitude over the period (data not shown).

The precipitable water has been calculated for Phases A and B and is shown in Table 1. There was a decrease in precipitable water from 3.8 g cm^{-2} during Phase A to 2.6 g cm^{-2} during Phase B. However, as mentioned, this change may have been caused by the influence of the large-scale high pressure acting over the region.

The synoptic geopotential and meridional wind component charts obtained from the US National Meteorological Center for the two phases of RBLE-II are shown in Figure 3. During phase A when measurements were made at the forest site, Figure 3a shows that the height of the 1500 hPa geopotential surface was 1540 m, and Figure 3b indicates a weak meridional component of the wind of approximately 2 m s^{-1}. This synoptic pattern was very similar to the one observed during Phase B, when measurements were made at the pasture, although some influence of high pressure can be seen on 22 July (Figure 3c) and Figure 3d shows that there was a weak wind from the north on that day.

RESULTS

The analysis of the atmospheric boundary layer distinguishes between daytime and night-time cases, as different physical process are involved.

NOCTURNAL BOUNDARY LAYER (NBL)

For this analysis we use data collected by tethered balloon at 20.00, 23.00, 02.00 and 0500 h. Table 2 shows the main characteristics of the development of the nocturnal boundary layer at the forest and pasture sites. In the literature, there is no consensus about the best way to determine the height of the nocturnal boundary layer, but criteria commonly used are the height where the gradient of the virtual potential temperature (θ_v) is null, or the height where the turbulence has ceased (Stull, 1988). However, for the same temperature profile, Garratt (1992) has shown that, for different criteria, the height obtained will be different. In this study, we define the height of the nocturnal boundary layer as the height where the gradient of θ_v is null or less than 0.01 K m^{-1}. The strength of the inversion is defined as the difference between θ_v at the top of the nocturnal boundary layer and its surface value.

Figure 3 Synoptic charts of the height of the 1500 hPa geopotential surface and the meridional component of the wind during RBLE-II: (a) and (b) for the Phase A forest measurement period; (c) and (d) for Phase B, when measurements were made at the pasture.

In Figure 4, the nocturnal evolution of the virtual potential temperature profile is shown for the night of 4 July (forest) and 19 July (pasture). For the forest case, at 20.00 h this nocturnal layer is well developed, showing a height of 190 m with a thermal inversion of 6.4 K. As the nocturnal radiative cooling continues, the layer becomes deeper, reaching 210 m at 23.00 h, 260 m at 02.00 h and 385 m at 05.00 h. These values are slightly higher than observations from Martin *et al.* (1988) for Central Amazonia. During this evolution, the thermal inversion increased from 7.2 K at 23.00 h to 8.5 K at 05.00 h. The virtual potential temperature has decreased from 305.7 K (at 20.00 h) to 304.1 K, around the time of sunrise (05.00 h). The largest cooling rate observed was 1.1 K h^{-1} between 20.00 and 23.00 h. In the pasture, although there is the same general pattern, the influence of the surface is very strong, modifying the overall values: at 20.00 h the height of the nocturnal boundary layer is 140 m with a virtual potential temperature of 305.3 K. By 23.00, the height has increased to 150 m, 200 m (at 02.00) and finally 240 m (at 05.00 h). The strength of the nocturnal inversion increases from 8.5 K (at 20.00 h) to 11.6 K (at 05.00 h): meanwhile the average virtual potential temperature has dropped from 305.3 K to 303.9 K. The cooling rate was observed to be around 1.4 K h^{-1}.

CONVECTIVE ATMOSPHERIC BOUNDARY LAYER (CBL)

The data-set used in this analysis were radiosoundings collected at 08.00, 11.00, 14.00 and 17.00 h. The vertical resolution of radiosounding is not as good as that of the tethered balloon profiles, but the top of the CBL, marked by a discontinuity in the virtual potential temperature profile can usually be clearly seen.

Figure 5 shows typical profiles of virtual potential temperature over the forest on 5 July and over the pasture on 22 July at 17.00 h. The height of the CBL was determined from visual inspection of the virtual potential temperature profiles. The height of the CBL at the forest site has been estimated to be 200 m at 08.00 h, growing abruptly to 580 m at 11.00 h (the rate of growth being 127 m h^{-1}). At 14.00 h the height is 1150 m and reaches a final height (1250 m) at 17.00 h. During the afternoon the CBL grows very little. The average layer virtual potential temperature

Table 2 Principal characteristics of nocturnal boundary layer at the forest and pasture. height (h) of the top of boundary layer, virtual potential temperature (θ_v) at the top of boundary layer and the strength of nocturnal boundary layer ($\Delta\theta_v$)

	Forest			Pasture		
Local time h	Height m	θ_v K	$\Delta\theta_v$ K	Height m	θ_v K	$\Delta\theta_v$ K
20.00	190	305.7	6.4	140	305.1	8.5
23.00	210	304.6	7.2	150	303.9	9.2
02.00	260	303.9	7.8	200	303.8	10.6
05.00	385	304.1	8.5	240	303.9	11.6

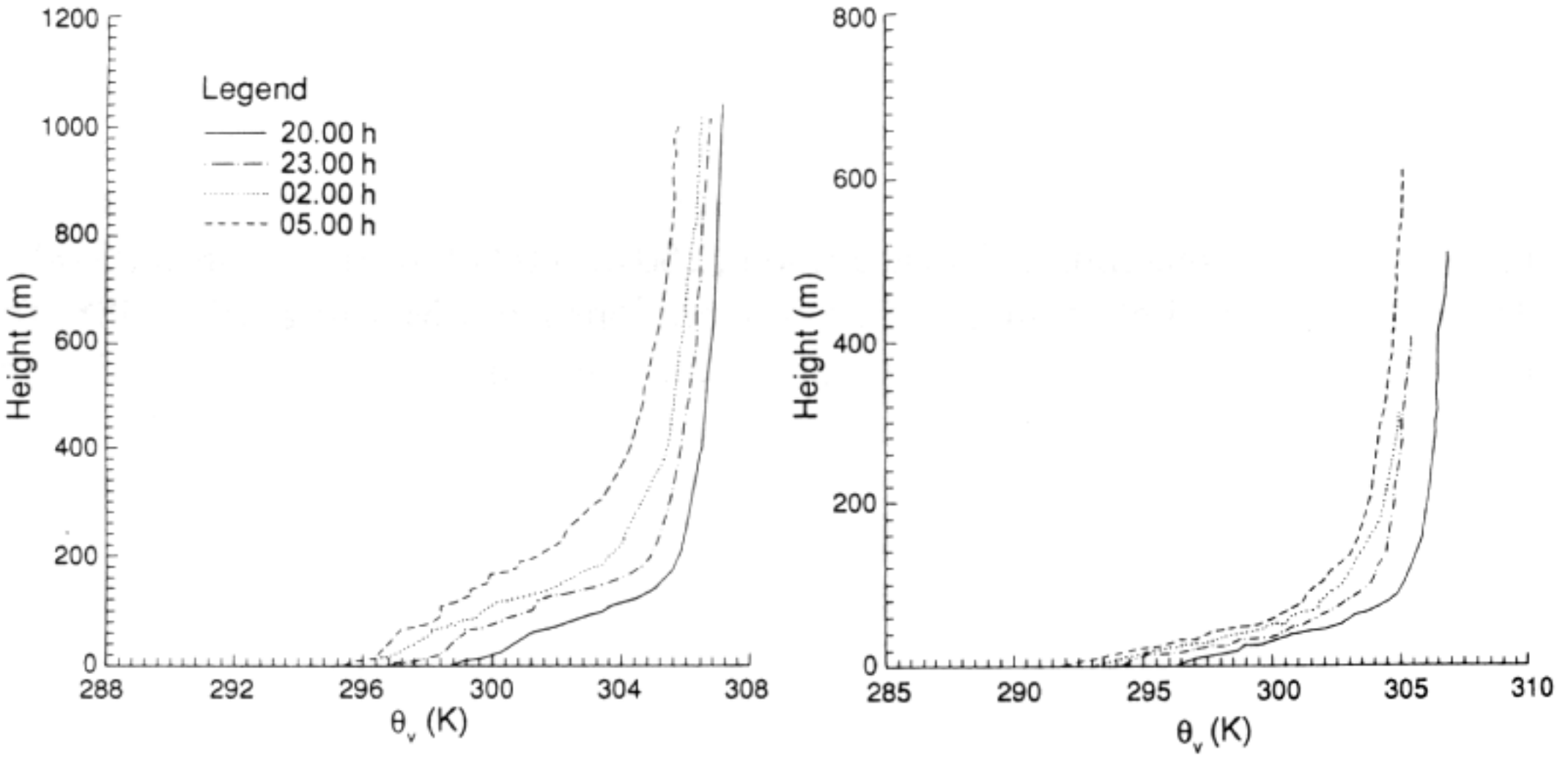

Figure 4 Nocturnal evolution of the virtual potential temperature (θ_v) on the nights of July 4 (left) and July 19 (right)

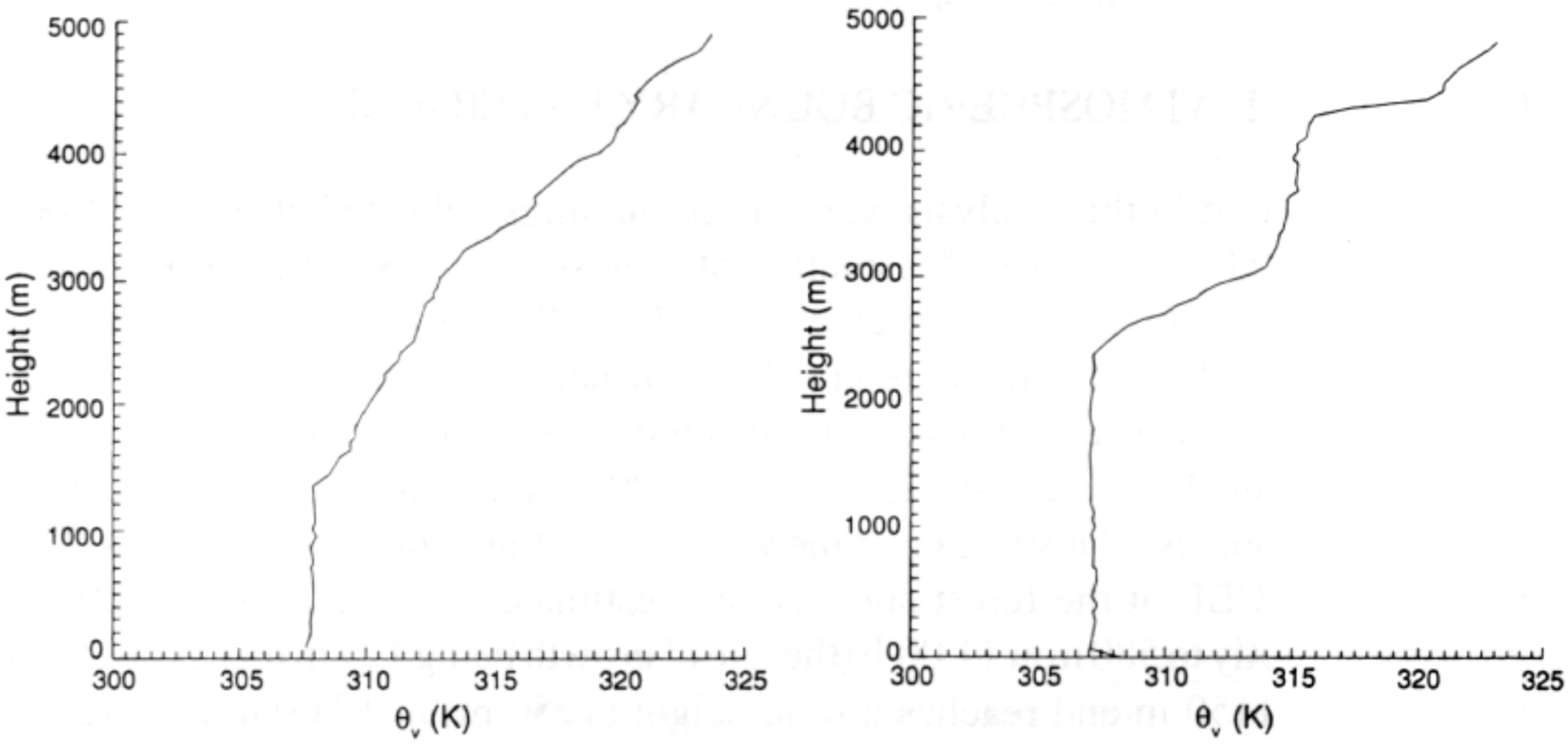

Figure 5 Typical late afternoon profiles of virtual potential temperature (θ_v) observed at the forest site (left) and the pasture site (right)

is 299.8 K during the early morning sounding (08.00 h) and reaches a final value of 307.2 K in the afternoon. The heating rate is high in the morning (1.6 K h^{-1}), when the nocturnal boundary layer is broken up by the surface heating. Later on, the heating rate is less (0.8 K h^{-1}) until 14.00 h, when the heating rate becomes stationary. In spite of the reduced surface heating in the late afternoon, the layer is still warmed by the entrainment flux of hot and dry air from above the CBL. Some authors (e.g. Tennekes, 1973; Driedonks, 1982) have considered the temperature gradient above the inversion as time-invariant, relating its change to large-scale variations. However, in the present case, this slope has a small time dependence,

slowly increasing with time: at 8.00 h it is 18 K km^{-1} and it increases to 3.3 K km^{-1} at 17.00 h. These general observations of CBL height are similar to the observations reported by Martin *et al.* (1988).

Table 3 summarises the structure of the CBL for forest and pasture conditions. The pasture analysis shows that at 08.00 h the height of CBL is lower than for forest (110 m), although it has a fast growth rate (493 m h^{-1}) up to 11.00 h, when the height has been estimated to be 1590 m. The final height is around 2220 m at 17.00 h. The average layer virtual potential temperature increases from 298.6 K to 305.6 K at 11.00 h (the rate of increase is 2.3 K h^{-1}). The pasture dataset also shows a time variation of the gradient of virtual potential temperature above the CBL, from 3.6 K km^{-1} in the morning up to 8.0 K km^{-1} at 17.00 h. Figure 6 shows a schematic diagram of the atmospheric boundary layer structure summarising these observations.

Table 3 Principal characteristics of convective boundary layer at the forest and pasture: height of the top of convective boundary layer, temperature gradient above the top of boundary layer (S_o) and average virtual potential temperature of the layer (θ_v)

	Forest			Pasture		
Local time h	Height m	S_o K km^{-1}	$\Delta\theta_v$ K	Height m	S_o K km^{-1}	$\Delta\theta_v$ K
08.00	200	1.8	298.8	110	3.6	298.6
11.00	580	2.5	304.5	1590	5.0	305.6
14.00	1150	3.0	306.9	2100	6.3	307.1
17.00	1250	3.3	307.2	2220	8.0	307.4

CONCLUSIONS

Although the ABL measurements made in RBLE-II were not made simultaneously over the two different surface types, some insights can be gained from analysing and comparing their structure. The greater depth of the nocturnal boundary layer at the forest site may be due to the influence of mechanical turbulence. At night the forest's high value of aerodynamic roughness induces a vertical diffusion which can deepen the nocturnal layer. The pasture site is aerodynamically smoother and so the downward turbulent diffusion will be much less, resulting in a lower surface temperature. The strength of thermal inversion is, consequently, higher over the pasture (48.3 K km^{-1}) than over the forest (22.4 K km^{-1}). The development of the convective boundary layer is stronger over the pasture than over the forest. The influence of the surface (through the sensible heat flux) is important but may be not enough to explain the difference completely. The deforestation management policy in the Ji-Paraná area leads to the creation of areas with strips of pasture and forest

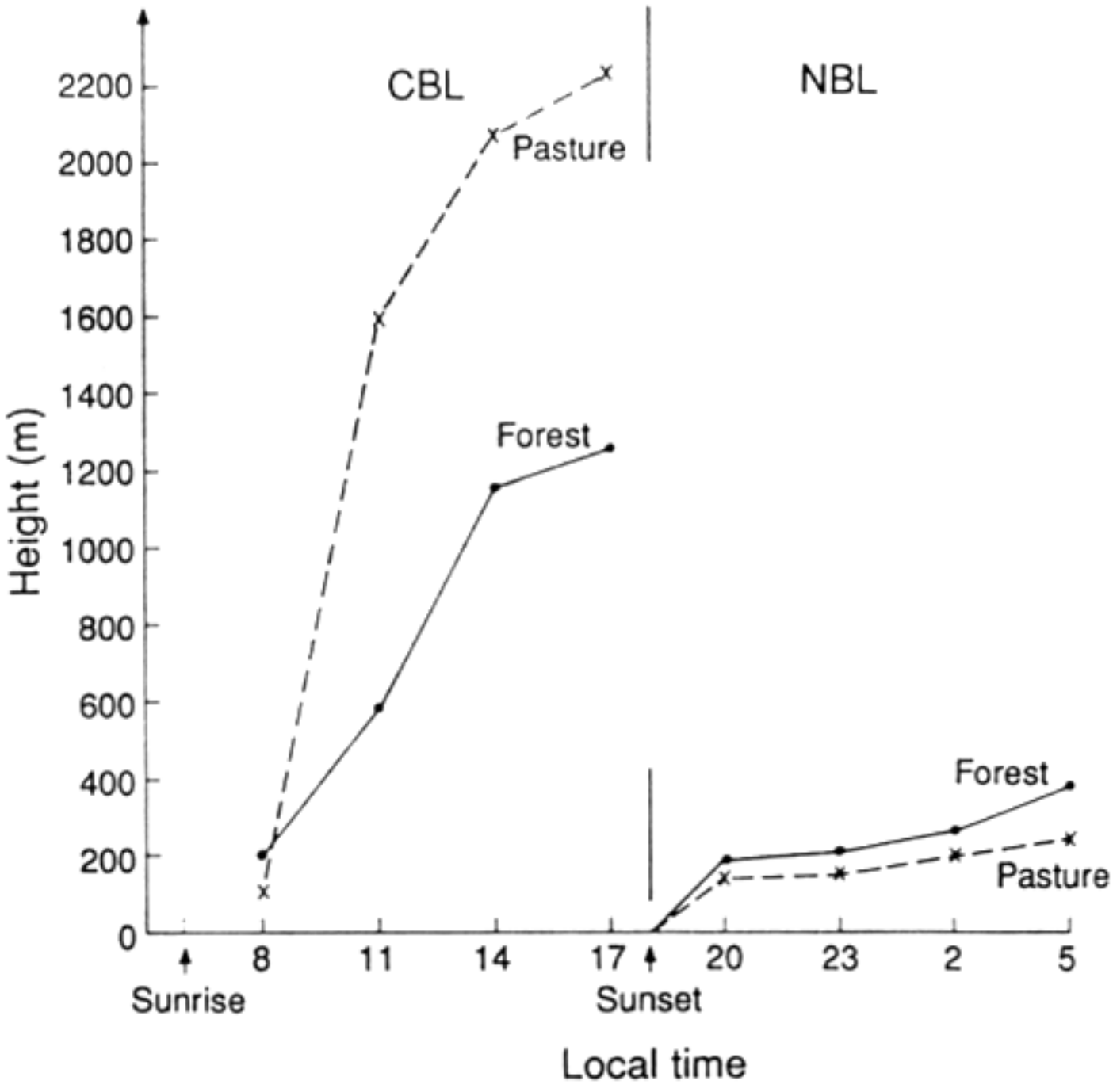

Figure 6 Schematic diagram of the ABL based on the composite observed data from RBLE-II

side-by-side and this contrast in vegetation (and the associated contrasting energy budgets) may lead to the generation of secondary thermal circulations. It seems that energy advection may occur from the wet and colder (forest) to the dry and warmer area (pasture), rapidly breaking up the nocturnal inversion. Such advection can explain the abrupt growth of the CBL at the pasture site during the early morning and is discussed further by Fisch *et al.* (1996).

ACKNOWLEDGEMENTS

The authors would like to express their thanks to all Brazilian and British participants of ABRACOS and RBLE-II who were involved in data collection at Ji-Paraná. RBLE-II was partially funded by Fundação de Amparo à Pesquisa do Estado de São Paulo (FAPESP) and Conselho Nacional Científico e Tecnológico (CNPq). One of the authors (G. Fisch) was funded by the Coordenadoria de Aperfeiçoamento de Pessoal de Nível Superior (CAPES) to carry out analysis at the Institute of Hydrology in the United Kingdom during 1993. Special thanks go to our colleagues J.H.C. Gash, J.M. Roberts, I.R. Wright and A.Culf (IH) and A. Beljaars (KNMI) for their help in preparing this paper. The authors would like to express their gratitude to the reviewers for their useful suggestions.

REFERENCES

Dickinson, R.E., Henderson-Sellers, A., Kennedy, P.J. and Wilson, M.F. 1984. Biosphere-Atmosphere Transfer scheme (BATS) for the NCAR community climate model, NCAR Technical Note TN-275+STR, 69 pp.

Dickinson, R.E. and Henderson-Sellers, A. 1988. Modelling tropical deforestation. a study of GCM land-surface parameterizations. *Q. J. Roy. Met. Soc.* **114**, 439-462.

Driedonks, A.C.M. 1982. Model and observations of the growth of the atmospheric boundary layer. *Bound.-Layer Met.* **23**, 283-306.

Fisch, G., 1995. Camada Limite Amazônica. aspectos observacionais e de modelagem. PhD Thesis, INPE, São José dos Campos, Brazil.

Fisch, G., Culf, A.D., and Nobre, C.A. 1996. Modelling convective boundary layer growth in Amazonia. This volume.

Garratt, J.R. 1992. *The atmospheric boundary layer*. Cambridge University Press, 316 pp.

Gash, J.H.C., Nobre, C.A., Roberts, J.M. and Victoria, R.L. 1996. An overview of ABRACOS. This volume.

Henderson-Sellers, A., Dickinson, R.E., Durbigde, T.B., Kennedy, P.J., McGuffie, K. and Pitman, A.J. 1993. Tropical deforestation modelling local to regional scale climate change. *J. Geophys. Res.* **98**, 7289-7315.

Lean, J. and Warrilow, D.A. 1989. Simulation of the regional climate impact of Amazon deforestation. *Nature* **342**, 411-413.

Lean, J. and Rowntree, P.R. 1993. A GCM simulation of the impact of Amazonian deforestation on climate using an improved canopy representation. *Q. J. Roy. Met. Soc.* **119**, 509-530.

Lyra, R., Druilhet, A., Benech, B. and Bouka Biorna, C. 1992. Dynamics above a dense equatorial rain forest to the free atmosphere. *J. Geophys. Res.* **97**, 12953- 12966.

Manzi, A.O. 1993. Introduction d'un schéma des tranferts sol-vegetation-atmosphère dans un modèle de circulation générale et application à la simulation de la deforestation Amazonienne. PhD Thesis, Paul Sabatier University, Toulouse (France), 230 pp.

Martin, C.M., Fitzjarrald, D.R., Garstang, M., Oliveira, A.P. de, Greco, S. and Browell, E. 1988. Structure and growth of the mixing layer over the Amazonian rain forest. *J. Geophys. Res.* **93**, 1361-1375.

McWilliam, A.-L.C., Cabral, O.M.R., Gomes, B.M., Esteves. J.L. and Roberts, J.M. 1996. Forest and pasture leaf-gas exchange in South-West Amazonia. This volume.

Nobre, C.A., Sellers, P.J. and Shukla, J. 1991. Amazonian deforestation and regional climate change. *J. Climate* **4**, 957-988.

Noilhan, J. and Planton, S. 1989. A simple parameterization of land surface process for meteorological models. *Mon. Weath. Rev.* **117**, 536-549.

Sellers, P.J., Mintz, Y., Sud, Y.C. and Dalcher, A. 1986. A simple biosphere model (SiB) for use within the General Circulation Models. *J. Amos. Sci.* **43**, 505-531.

Shuttleworth, W.J., Gash, J.H.C., Lloyd, C.R., McNeil, D.D., Moore, C.J. and Wallace, J.S. 1988. An integrated micrometeorological system for evaporation measurements. *Agric. For. Met.* **43**, 295-317.

Stull, R.B. 1988. *An introduction to boundary layer meteorology*. Kluwer Academic Publishers, Dordrecht, 666 pp.

Tennekes, H. 1973. A model for the dynamics of the inversion above a convective boundary layer. *J. Atmos. Sci.* **30**, 558-567.

Wright I.R., Nobre, C.A., Tomasella, J., da Rocha, H.R., Roberts, J.M., Vertamatti, E., Culf, A.D., Alvalá, R.C., Hodnett, M.G. and Ubarana, V. 1996. Towards a GCM surface parameterisation for Amazonia. This volume.

RESUMO

Observações do desenvolvimento de camadas limites atmosféricas sobre regiões de floresta tropical e pastagem são apresentadas. Estas medidas foram obtidas no Experimento da Camada Limite de Rondônia — Fase II, realizado na região de Ji-Paraná (sudoeste da Amazônia), durante o mês de julho de 1993. O conjunto de dados consiste em perfis atmosféricos medidos a partir de balão cativo, radiossondagem e de medidas de fluxos turbulentos à superfície. Os resultados mostram que a camada limite convectiva desenvolvida sobre a área de pastagem pode atingir alturas de até 2.200 m ao final da tarde, valores estes superiores aos observados sobre a floresta (1.250 m). A camada limite estável noturna é mais profunda sobre a floresta (385 m) do que sobre a pastagem (240 m). Os mecanismos atmosféricos que determinam estas características são discutidos.